ICANS-VI

INTERNATIONAL COLLABORATION ON ADVANCED NEUTRON SOURCES

June 27 - July 2, 1982

CRYSTAL ANALYZER TOF SPECTROMETER (CAT) FOR HIGH ENERGY INCOHERENT NEUTRON SCATTERING

Noboru Watanabe and Susumu Ikeda

National Laboratory for High Energy Physics
Oho-machi, Tsukuba-gun, Ibaraki-ken, 305, Japan

Kenzo Kai

The Research Institute for Iron, Steel and Other Metals
Tohoku University, Sendai, 980, Japan

ABSTRACT

This paper reports the design and performances of a high resolution crystal analyzer spectrometer which has been built and operated at KENS. Energy resolution of the instrument is $\Delta\varepsilon/\varepsilon = 0.02 \sim 0.03$ in the range of energy transfer $\varepsilon = 0.05 \sim 1$ eV. With this spectrometer, local mode of hydrogens in various metallic hydrides have been measured. In case of TiH_2 or ZrH_x, higher harmonics of the optical peaks have been detected up to 5th orders with their fine structures. Higher order peaks of $TaH_{0.5}$ have also been detected. Optical mode in hydrogenated metallic glass of $NiTiH_{0.5}$ has been measured and compared with that in crystalline sample.

CRYSTAL ANALYZER TOF SPECTROMETER (CAT) FOR HIGH ENERGY INCOHERENT NEUTRON SCATTERING

Noboru Watanabe and Susumu Ikeda
National Laboratory for High Energy Physics
Oho-machi, Tsukuba-gun, Ibaraki-ken, 305, Japan

Kenzo Kai
The Research Institute for Iron, Steel and Other Metals
Tohoku University, Sendai, 980, Japan

1. INSTRUMENT

A high resolution crystal spectrometer has been built and operated at KENS. The instrument makes possible the measurement of incoherent neutron scattering with large energy transfer in the range $\varepsilon = 0.05 \sim 1$ eV, with resolution of about $\Delta\varepsilon/\varepsilon = 0.02 \sim 0.03$ in the entire range of energy transfer[1]. The instrument is an inverted geometry type; the scattered neutrons are detected at a fixed energy by a large analyzer crystal, while the incident neutron energy is determined from the measured total time of flight, t, using the following relation,

$$t = \frac{L_i}{V_i} + \frac{L_f}{V_f} , \qquad (1)$$

where L_i, L_f, V_i, and V_f are incident (i) and scattered (f) flight paths lengths and neutron velocities, respectively.

In this type of spectrometer, generally speaking, uncertainty in the second term becomes large due to the finite extent of sample, analyzer, and detector. This reflects on the first term through the relation in equation (1) and results in the poor definition of the incident energy. If we put the sample and the detector on a plane, and set the analyzer parallel to this plane as shown in Fig. 1(a), then two dimensional focussing is realized in time of flight between sample and detector. This focussing geometry make it possible to improve the energy resolution without sacrificing the geometric counting efficiency. A prototype spectrometer of this type was developed and operated at Tohoku linac[2-4]. In the new machine at KENS, signal to background ratio has been largely increased with an improved energy resolution[1]. Momentum transfer, Q,

is rapidly increased with energy transfer, ε, due to the low final energy, but the spectrometer will be useful for the measurements of the local mode of hydrogens in metalic hydrides, for the molecular spectroscopy, etc., where the value of Q is not crucial and the Q-dependence is not so important. Similar instruments were operated also at the pulsed neutron facilities of Harwell linac[5], ZING-P' at Argonne[6], and WNR, at Los Alamos[7].

Figure 1(b) shows the spectrometer configuration. The instrument has been installed at H-7 beam hole which views the surface of a moderator (polyethylene slab at room temp.) perpendicularly. Maximum beam size at sample position is 7 cm^W x 7 cm^H. In order to minimize the ambiguity of the incident flight path length, a plane sample is set perpendicularly to the beam at L_1 = 5.299 m. The analyzer crystal is a 10 cm x 10 cm pyrographite (mosaic spread 1.2°). Bragg angle of $\theta_B \sim 43°$ is used, and 002 reflection corresponds to E_f = 4 meV. Eight He-3 proportional counters, 1/2 inches in diam. and 12 inches in active length filled to 20 atoms pressure, are set in horizontal direction to form a detector plane. In the present configuration, center line distance between sample and analyzer, and that between analyzer and detector are 36 cm respecively which correspond to inter plane distance a = 24.2 cm. A beryllium filter (9.5 cm^H x 12 cm^W x 15 cm^L) cooled to liquid nitrogen temperature is used between analyzer and detector with a post cross collimator made of cadmium, in order to eliminate neutrons due to higher order reflections. Sample-analyzer-detector system is buried in a shield box of 2 cm thick B_4C and 25 cm thick borated resin wall.

2. ENERGY RESOLUTION

Extensive studies of the energy resolution were performed by a Monte Carlo computer simulation for sample-analyzer-filter detector system. Figure 2(a) shows the effect of the mosaic spread, β, in the analyzer crystal on the time distribution of the scattered neutrons. This indicates that mismatch in time focussing due to the finite value in β is not significant in this spectrometer. The most probable value

of t_f is determined to be t_f = 821 μsec from this result.

Figure 2(b) shows the calculated energy spectrum of the scattered neutrons. The width is fairly wide which is consistent with measurement, and from this distribution, mean value of E_f is determined to be $\bar{E}_f$ = 3.9 meV.

The effect of the finite size and circular cross section of the detector was also studied. Even with 1/2" diam. counter, the effect seems significant, and if necessary we can improve the resolution by placing a proper cadmium mask, with a sacrifice in counting efficiency by about 30 %. Calculated values of the total and partial resolution are shown in Fig. 3 as a function of energy transfer.

3. PERFORMANCE

In order to test the performance of the spectrometer, local vibration mode of hydrogens in various metalic hydride samples has been measured[1),8)]. In Fig. 4(a) is shown a typical raw data of TOF spectrum obtained from TiH_2 at room temperature which demonstrates the extremely low background level compared to the results obtained at other laboratories. Even at the time corresponding to $\varepsilon = \infty$, background is low enough to observe a small step increase in the spectrum. Figure 4(b) shows the energy spectrum which demonstrates the higher resolution of the instrument. Higher harmonics are clearly observed up to 5th order with their fine structures.

$ZrH_{1.41}$ and $ZrH_{1.93}$ have been measured and the results are shown in Fig. 5. The locations of the peaks are listed in Table 1 with those obtained for TiH_2 and $TaH_{0.5}$. It is obvious that the frequencies for higher harmonics are shifted by appreciable amounts from the respective harmonic positions, and from these frequency shifts we can determine the anharmonicity parameters of the hydrogen potential. The striking feature of the fine structures in the higher harmonics is that the separation or the split of the subpeaks in the respective orders becomes more pronounced

at higher harmonics. In the fundamental peak of $ZrH_{1.93}$, there are two sub-peaks at about 138 meV and 145 meV with a shoulder at about 154 meV. The results is consistent with the reported values by Couch, et al.[9] There exists a distinct difference between the fine structures of $ZrH_{1.41}$ (cubic) and those of $ZrH_{1.93}$ (tetragonal), especially in the 2nd harmonics.

Table 1 Peak Positions of Localized Modes

	1st (meV)	2nd (meV)	3rd (meV)	4th (meV)	5th (meV)
$ZrH_{1.93}$ (300 K)	138 145 154	257 274 293	389 415	500 531	644 677
$ZrH_{1.41}$ (300 K)	137 141 146	260 274 297	394 433	493 531 565	644 666
TiH_2 (300 K)	139 148 154 171	263 280 304	394 405 433	523 565	678 740
$TaH_{0.5}$ (300 K)	122 130 162 167	233 236 277 318			
$TaH_{0.5}$ (30 K)	124 130 161	225 239 277			

Figure 6 shows the results of $TaH_{0.5}$. In $TaH_{0.5}$ at room temperature, the lower fundamental peak ($\sim$ 120 meV) has a shoulder at about 130 meV, and the higher fundamental ($\sim$ 160 meV) splits into two peaks. Hempelmann, et al.[10] have measured $TaH_{0.08}$ and fitted the higher fundamental peak by two Gaussians. The present results are qualitatively consistent with theirs. They have found the second harmonics of the lower fundamental at about 227 meV which may correspond to our peak at 223 meV. In the present spectrum, many extra peaks are observed above this energy. Some of them may be attributed to the multi-phonon contribution of the fundamentals. Assignement of the peaks are now in progress. The results at low temperature are also shown in the figure.

Hydrogenated metallic glass of $NiTi_2H_{0.5}$ has also been investigated[11], in which hydrogen atoms reside in the central hole of polyhedral unit structures of metallic atoms. The results are shown in Fig. 7 where the measured spectra of TiH_2, $NiTi_2H_{0.9}$ and $NiTi_2H_{0.5}$ crystals are also displayed for comparison. The striking new result is the observation of well defined higher harmonics of the local mode in glassy metallic hydride. Higher harmonics in the glassy sample are clearly observed up to 4th or 5th order at low temperature as in crystalline sample, while a rapidly damping occurs beyond 3rd harmonics at room temperature.

Table 2 Locations and Line Widths of 1st, 2nd and 3rd Harmonics

	1st level		2nd level		3rd level	
	$\hbar\omega$	FWHM	$\hbar\omega$	FWHM	$\hbar\omega$	FWHM
a-$(NiTi_2)H_{0.5}$	143±2	74±5	275±3	106±10		
c-$(NiTi_2)H_{0.5}$	150±2	36±5	286±3	67±10	410±8	90±20
c-$(NiTi_2)H_{0.9}$	144±2 155±2	47±5	286±3	90±10	412±8	140±20
TiH_2		31±1	264±3 285±3	55±5	394±8 428±8	96±10

unit: meV

The location and width of the optic peaks are summarised in Table 2. Note that the low-energy shoulder appearing at $\hbar\omega \leq 100$ meV in the crystalline $NiTi_2H_{0.5}$ is also found in the glassy state. This shoulder seems to be contributed from hydrogen atoms in the possible octahedral site as in crystalline state[12]. Details will be given in separate a rticles.

References

1) S. Ikeda, N. Watanabe, K. Kai and S. Yamaguchi, KENS Report III, KEK Internal (1982).

2) N. Watanabe, M. Furusaka and M. Misawa, Research Rep't. Lab. Nucl. Sci., Tohoku Univ. 12 (1979) 72 (in Japanese).

3) M. Furusaka, N. Watanabe and H. Asano, ibid. 12 (1979) 83 (in Japanese).

4) N. Watanabe and M. Furusaka, KENS Report I, KEK Internal 80-1 (1980) 181.

5) D. H. Day and R. N. Sinclair, J. Chem. Phys. 55 (1971) 2870.

6) K. Sköld, K. Crawford and H. Chen, Nucl. Instrum. Methods 145 (1977) 117.

7) J. Eckert, R. N. Silver, A. Soper, P. J. Vergamini, J. Goldstone, A. Larson, P. A. Seeger and J. Yarnell, Proc. ICANS-IV (1981) 434.

8) S. Ikeda, N. Watanabe and K. Kai, Kens Report III, KEK Internal (1982).

9) J. G. Couch, O. K. Harling and L. C. Clune, Phys. Rev. B 4 (1981) 159.

10) R. Hempelmann and D. Richter, Z. Phys. B - Condensed Matter 44 (1981) 159.

11) K. Kai, S. Ikeda, N. Watanabe and K. Suzuki, KENS Report III, KEK Internal (1982).

12) H. Buchner, M. A. Gutijar, K-D. Beccu and H. Säufferer, Z. Metalkd. 63 (1972) 497.

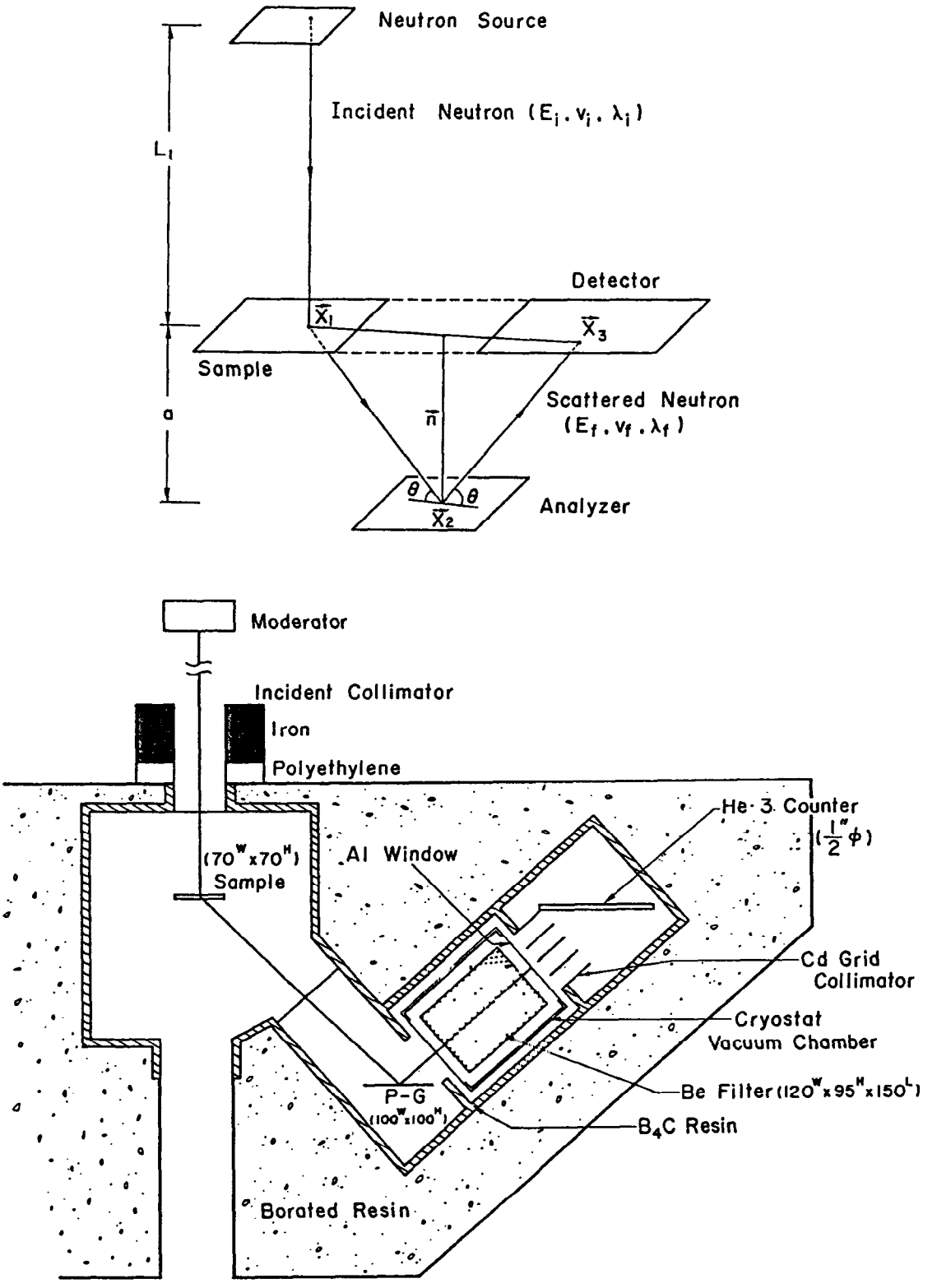

Fig. 1 Principle (a) and configuration (b) of the spectrometer

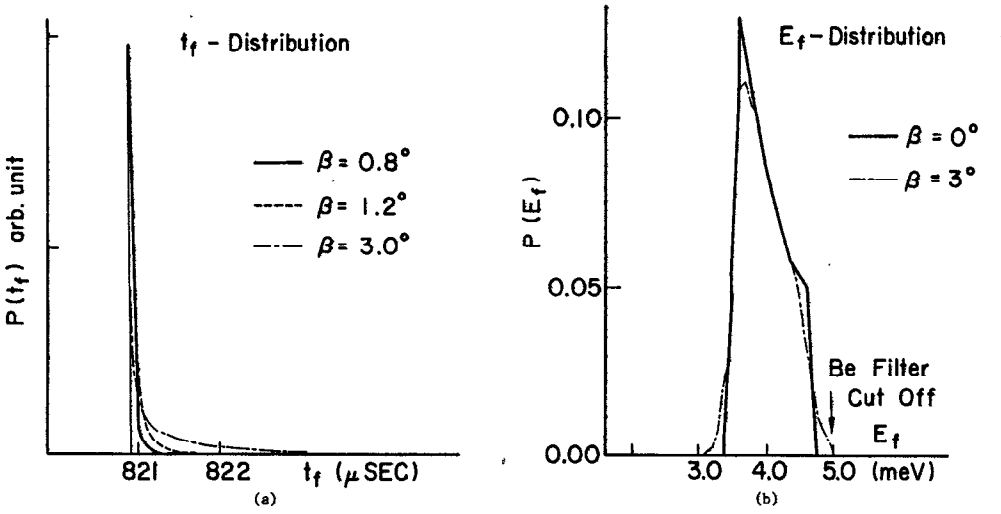

Fig. 2. Time distribution of detected neutrons due to finite mosaic spread of analyzer crystal (a) and energy distribution of detected neutrons.

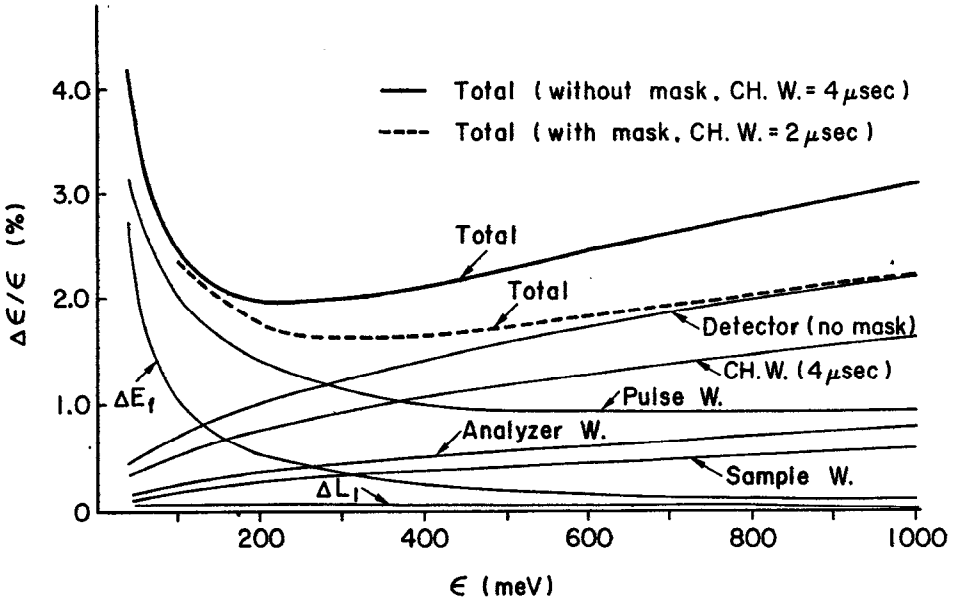

Fig. 3. Total and partial energy resolution.

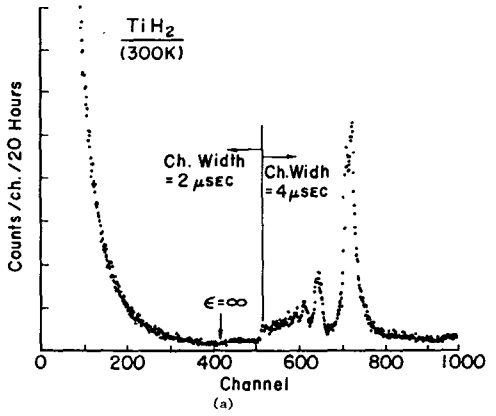

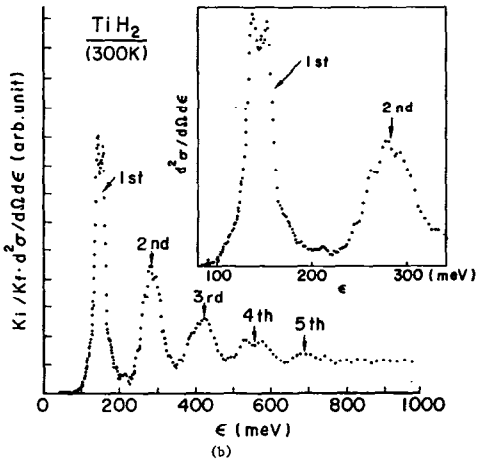

Fig. 4

Raw TOF spectrum (a) and double differential cross section (b) of TiH_2.

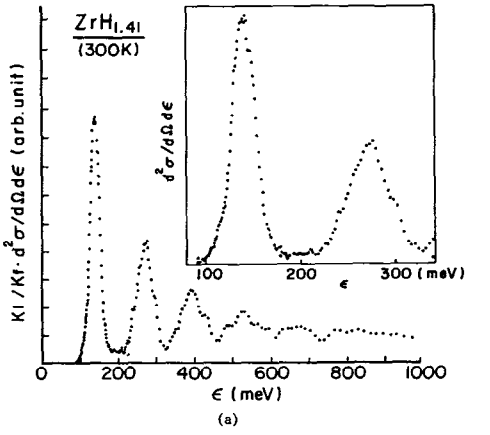

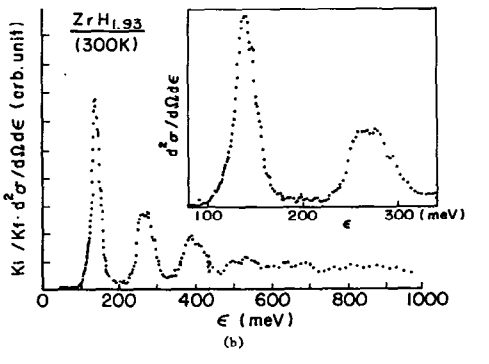

Fig. 5

Double differential cross section of $ZrH_{1.41}$ (a) and $ZrH_{1.93}$ (b)

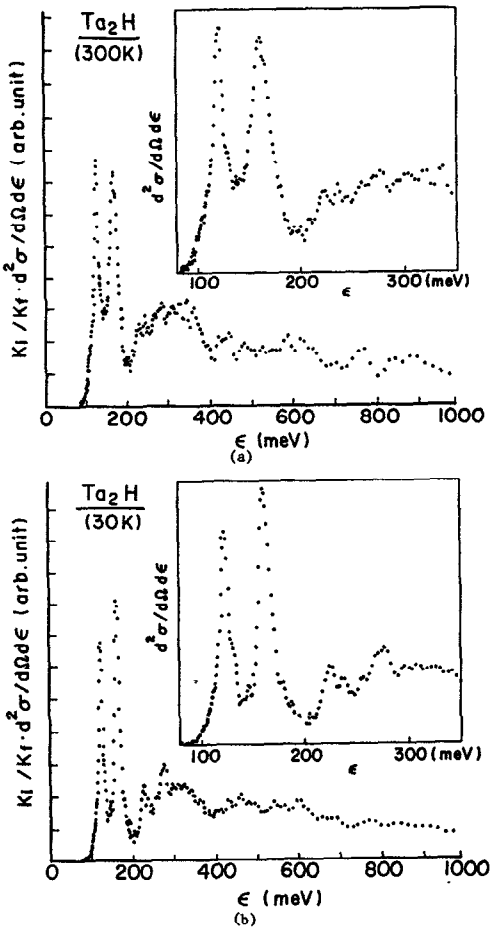

Fig. 6

Double differential cross section of Ta_2H at room temperature (a) and at 30 K (b).

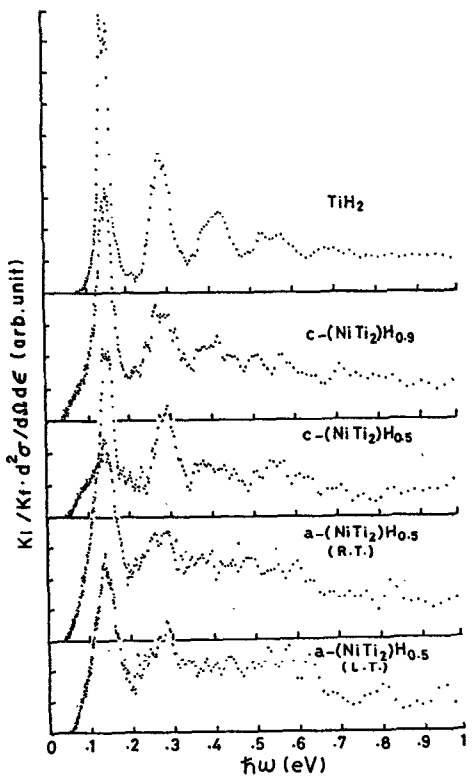

Fig. 7

Double differential cross section of amorphous $Ni_{0.33}Ti_{0.67}H_{0.5}$ compared with those of $Ni_{0.33}Ti_{0.67}$, $H_{0.5}$, $NiTi_2H_{0.9}$ and TiH_2 crystals.